

## Supporting Information for: Molecular Adsorption and Resonance Coupling at the Colloidal Gold Nanoparticle Interface

Tony E. Karam and Louis H. Haber

Department of Chemistry, Louisiana State University, Baton Rouge, Louisiana 70803

### Second harmonic generation data and fits

The adsorption isotherms obtained from the SHG data are fit using an extended modified Langmuir model that takes into account the signal generated from the free dye molecules in water. The total SHG signal is considered to be the sum of the three different contributions including the adsorption of molecules on the surface of gold nanoparticles, the offset from gold nanoparticles in water, and the signal generated from free dye molecules in water. The later term is considered negligible in the case of the adsorption studies on the surface of polystyrene microspheres. The total signal can be written as

$$SHG_{total} = A\left(\frac{N}{N_{max}}\right)^2 + B + Ma \quad (S1)$$

where  $N/N_{max}$  is obtained from the modified Langmuir formula,  $A$  is the SHG amplitude at the plateau,  $B$  is the offset term due to the SHG signal from gold nanoparticles in water without the addition of the dye solution,  $M$  is the concentration of free dye molecules in solution, and  $a$  is the slope obtained from plotting the SHG signal of dye molecules in water versus dye concentration. Figure S1 shows the SHG signal of the different dyes in water at different reduced concentrations, which is the ratio of the concentration over the maximum concentration value. The maximum concentrations used for malachite green, brilliant green, and methyl green are 1.8  $\mu$ M, 15  $\mu$ M, and 8  $\mu$ M respectively. It is shown that the SHG signals of the three dyes in water increase linearly, as expected for hyper Rayleigh scattering. The variation of  $M$  as a function of dye concentration,  $N_{max}$ , and  $K$  are determined using the best fits from the modified Langmuir model. In order to generate the adsorption isotherms, the data are corrected by subtracting the contribution of the free dye molecules in water from the total SHG signal.

By fitting the SHG data as described above using the extended modified Langmuir model, the site densities and the free energies of adsorption of the dye molecules to the surface of polystyrene microspheres are determined, as shown in Figure S2. The polystyrene sulfate microspheres are purchased from Polysciences and are diluted in nanopure water to a concentration of  $4.0 \times 10^8$  particles/mL for each SHG adsorption isotherm measurement. The experimental setup is the same as the one used for the gold nanoparticle measurements, with the same data analysis procedure. Using the extended modified Langmuir model, the free energy of adsorption of malachite green to the surface of  $1.06 \pm 0.03 \mu\text{m}$  polystyrene microspheres is  $-11.0 \pm 0.2$  kcal/mol and the maximum number of sites per particle is  $1.80 \pm 0.04 \times 10^6$  where each site occupies  $192 \pm 9 \text{ \AA}^2$ . These values are equivalent to the values obtained, under experimental uncertainty, using the modified Langmuir model, which neglects signal from free dye molecules. Using the modified Langmuir model, the corresponding adsorption energy is  $-11.1 \pm 0.4$  kcal/mol and the maximum number of sites is  $1.83 \pm 0.06 \times 10^6$  per particle where each site occupies  $193 \pm 6 \text{ \AA}^2$ . These results are very similar to values reported in the literature [1, 2]. In addition, brilliant green and methyl green molecules bind more strongly to the surface of the polystyrene microspheres than malachite green. The free energy of adsorption of brilliant green is  $-13.0 \pm 0.3$  kcal/mol with a maximum of  $1.61 \pm 0.06 \times 10^6$  sites per particle where each site occupies  $216 \pm 9 \text{ \AA}^2$ , using the extended modified Langmuir model fit. Using the modified Langmuir model, these corresponding values are  $-12.8 \pm 0.2$  kcal/mol,  $1.57 \pm 0.08 \times 10^6$  sites per particle, and  $220 \pm 13 \text{ \AA}^2$ , respectively. The free energy of adsorption of methyl green is  $-14.1 \pm 0.5$  kcal/mol with a maximum of  $1.26 \pm 0.10 \times 10^6$  sites per particle where each site occupies  $275 \pm 12 \text{ \AA}^2$ , using the extended modified Langmuir model fit. Using the modified Langmuir model, these corresponding values are  $-14.4 \pm 0.5$  kcal/mol,  $1.30 \pm 0.10 \times 10^6$  sites per particle, and  $267 \pm 15 \text{ \AA}^2$ , respectively. To our knowledge, no work has previously reported SHG results for brilliant green and methyl green adsorbing to polystyrene microspheres in water.

### **Polaritons and Fano-type resonances at the colloidal gold interface measured using absorption spectroscopy**

Extinction measurements of the  $80.0 \pm 6.1$  nm gold nanoparticles are performed at different malachite green and methyl green concentrations, in the same way described for the

brilliant green results shown in the paper. Figures S3 (a) and (b) display these spectra after subtracting the spectra of the dye solutions in water at the corresponding concentrations. A splitting of the plasmon peak is observed near the molecular resonances, with plasmon and molecular resonance coupling and spectral depletions as the dye concentrations are increased over the range studied in the SHG adsorption isotherm measurements. After subtracting the spectra of gold nanoparticles at the corresponding concentrations from the absorption spectra in Figure S3, the difference spectra are obtained and shown in Figure S4. The molecule and plasmon depletion fits are displayed in black dashed lines. The residual negative and positive peaks observed are due to a convolution of polaritons and Fano-type resonances. The peaks at higher wavelengths correspond to the lower energy polaritonic state  $|P-\rangle$  and the peaks at lower wavelengths correspond to the higher energy polaritonic state  $|P+\rangle$ , respectively. The energy differences between these two peaks are assigned as the Rabi splitting energies. The plasmon peak is depleted as the dye concentrations increase. Figure S5 is obtained after subtracting the corresponding depletion fits from the difference spectra in figure S4, with offsets added for comparisons. The polariton peaks in Figure S5 are fit using the double Gaussian equation S2 for the determinations of the peak positions, widths, intensities, and offset values. The results are summarized in table S1.

$$y = y_0 + A_1 \exp \left[ - \left( \frac{x - x_1}{w_1} \right)^2 \right] + A_2 \exp \left[ - \left( \frac{x - x_2}{w_2} \right)^2 \right] \quad (S2)$$

The chemical structures and the absorption spectra of malachite green, brilliant green, and methyl green are shown in Figures S6 and S7, respectively.

(a)	MG Conc	131 nM	251 nM	362 nM	465 nM	561 nM
	Plasmon Depletion	-1.4E-02 $\pm$ 2.0E-03	-2.2E-02 $\pm$ 1.2E-03	-3.0E-02 $\pm$ 3.1E-03	-4.4E-02 $\pm$ 2.1E-03	-5.9E-02 $\pm$ 1.1E-03
	Molecule Depletion	3.1E-03 $\pm$ 1.1E-03	-1.5E-02 $\pm$ 3.1E-03	-5.4E-02 $\pm$ 2.6E-03	-8.3E-02 $\pm$ 3.6E-03	-1.3E-01 $\pm$ 2.4E-03
	$y_0$	5.6E-04 $\pm$ 3.4E-04	5.9E-04 $\pm$ 1.2E-04	3.9E-04 $\pm$ 1.5E-04	4.7E-04 $\pm$ 1.3E-04	-1.3E-04 $\pm$ 1.2E-04
	$A_1$	1.9E-03 $\pm$ 3.2E-04	2.3E-03 $\pm$ 1.1E-04	2.6E-03 $\pm$ 1.4E-04	2.7E-03 $\pm$ 1.3E-04	2.87E-03 $\pm$ 1.17E-04
	$x_1$	660 $\pm$ 0.1	660 $\pm$ 0.1	650 $\pm$ 0.1	650 $\pm$ 0.1	650 $\pm$ 0.1
	$w_1$	29 $\pm$ 4	28 $\pm$ 2	26 $\pm$ 2	22 $\pm$ 1	24 $\pm$ 1
	$A_2$	-2.1E-03 $\pm$ 2.6E-04	-2.0E-03 $\pm$ 9.3E-05	-2.1E-03 $\pm$ 1.2E-04	-1.4E-03 $\pm$ 8.7E-05	-1.3E-03 $\pm$ 6.9E-05
	$x_2$	578 $\pm$ 0.1	578 $\pm$ 0.1	578 $\pm$ 0.1	580 $\pm$ 0.1	579 $\pm$ 0.1
	$w_2$	23 $\pm$ 3	23 $\pm$ 1	24 $\pm$ 2	19 $\pm$ 2	17 $\pm$ 1
(b)	BG Conc	1.3 $\mu$ M	2.5 $\mu$ M	3.5 $\mu$ M	4.5 $\mu$ M	5.45 $\mu$ M
	Plasmon Depletion	-7.9E-02 $\pm$ 1.2E-02	-1.0E-01 $\pm$ 2.7E-03	-1.4E-01 $\pm$ 2.3E-03	-1.8E-01 $\pm$ 3.4E-03	-2.3E-01 $\pm$ 2.9E-03
	Molecule Depletion	-1.2E-02 $\pm$ 3.5E-03	-1.6E-02 $\pm$ 4.2E-03	-7.5E-03 $\pm$ 5.1E-03	-1.0E-03 $\pm$ 2.0E-03	1.1E-02 $\pm$ 3.1E-03
	$y_0$	4.8E-03 $\pm$ 5.9E-04	2.2E-03 $\pm$ 4.1E-04	7.6E-03 $\pm$ 7.7E-04	4.5E-03 $\pm$ 8.2E-04	2.5E-03 $\pm$ 4.8E-04
	$A_1$	5.3E-03 $\pm$ 1.6E-04	5.3E-03 $\pm$ 1.9E-04	4.4E-03 $\pm$ 1.6E-04	6.1E-03 $\pm$ 4.3E-04	4.9E-03 $\pm$ 1.8E-04
	$x_1$	660 $\pm$ 0.1	660 $\pm$ 0.1	660 $\pm$ 0.1	670 $\pm$ 0.1	660 $\pm$ 0.1
	$w_1$	22 $\pm$ 1	21 $\pm$ 1	21 $\pm$ 1	26 $\pm$ 2	21 $\pm$ 1
	$A_2$	-5.8E-03 $\pm$ 4.4E-04	-6.4E-03 $\pm$ 1.8E-04	-7.1E-03 $\pm$ 5.0E-04	-8.6E-03 $\pm$ 2.1E-04	-6.6E-03 $\pm$ 2.9E-04
	$x_2$	570 $\pm$ 0.1	570 $\pm$ 0.1	570 $\pm$ 0.1	570 $\pm$ 0.1	570 $\pm$ 0.1
	$w_2$	23 $\pm$ 1	20 $\pm$ 1	22 $\pm$ 2	26 $\pm$ 5	20 $\pm$ 1
(c)	MetG Conc	1.17 $\mu$ M	2.26 $\mu$ M	3.25 $\mu$ M	4.20 $\mu$ M	
	Plasmon Depletion	-6.9E-02 $\pm$ 9.1E-03	-1.1E-01 $\pm$ 9.1E-03	-1.6E-01 $\pm$ 8.7E-03	-1.9E-01 $\pm$ 7.5E-03	
	Molecule Depletion	-2.8E-03 $\pm$ 9.0E-03	-2.6E-02 $\pm$ 9.0E-03	-2.9E-02 $\pm$ 1.2E-02	-3.4E-02 $\pm$ 1.4E-03	
	$y_0$	5.5E-03 $\pm$ 2.3E-04	1.4E-03 $\pm$ 1.1E-04	1.3E-03 $\pm$ 8.9E-05	1.3E-03 $\pm$ 2.5E-04	
	$A_1$	8.2E-04 $\pm$ 1.7E-04	9.1E-04 $\pm$ 1.7E-04	7.7E-04 $\pm$ 1.3E-04	1.9E-03 $\pm$ 1.4E-04	
	$x_1$	670 $\pm$ 0.1	670 $\pm$ 0.1	670 $\pm$ 0.1	670 $\pm$ 0.1	
	$w_1$	10 $\pm$ 3	12 $\pm$ 3	7 $\pm$ 2	13 $\pm$ 3	
	$A_2$	-4.9E-03 $\pm$ 1.2E-04	-1.8E-03 $\pm$ 1.2E-04	-1.2E-03 $\pm$ 6.4E-05	-1.4E-03 $\pm$ 1.1E-04	
	$x_2$	580 $\pm$ 0.1	580 $\pm$ 0.1	570 $\pm$ 0.1	570 $\pm$ 0.1	
	$w_2$	72 $\pm$ 2	28 $\pm$ 2	21 $\pm$ 2	31 $\pm$ 3	

Table S1: Resonance coupling fits of the polariton  $|P-\rangle$  and  $|P+\rangle$  peaks to a double Gaussian function provides the peak positions  $x_1$  and  $x_2$ , the peak widths  $w_1$  and  $w_2$ , the peak intensities  $A_1$  and  $A_2$ , and the offset  $y_0$  at different (a) malachite green, (b) brilliant green and (c) methyl green concentrations.

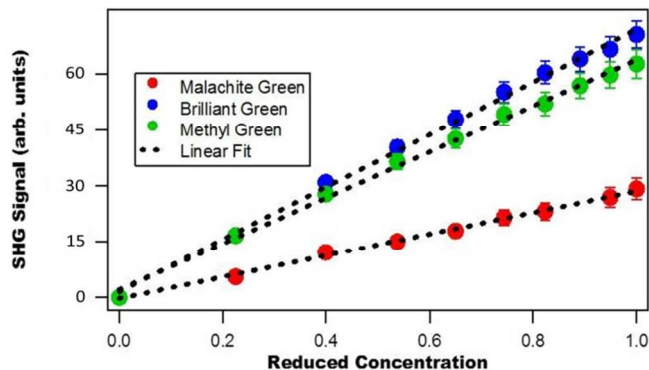


Figure S1. Second harmonic generation signal obtained from the addition of malachite green (red line), brilliant green (blue line) and methyl green (green line) to water. The signals are shown to increase linearly, as expected for hyper-Raleigh scattering.

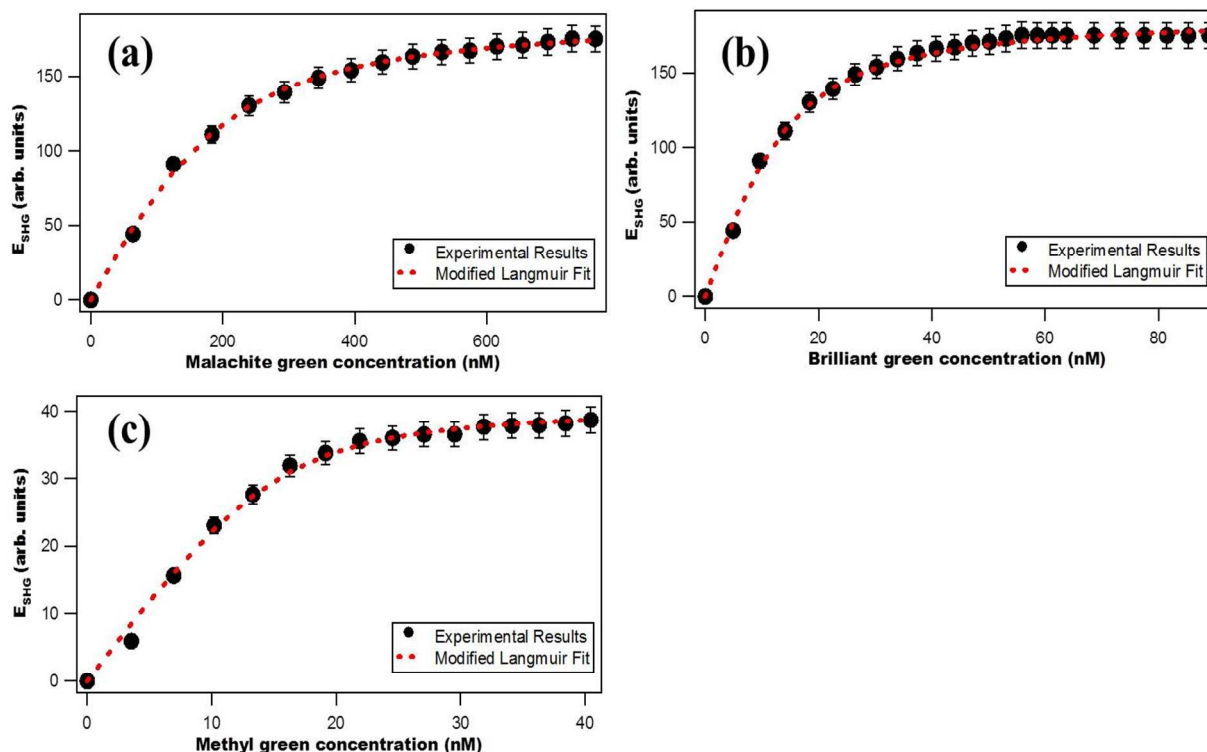


Figure S2. Adsorption isotherm results obtained from second harmonic generation data (black dots) from polystyrene microspheres as a function of (a) malachite green, (b) brilliant green, (c) and methyl green concentrations. The experimental data are compared with the best fits from the modified Langmuir model (dotted red lines).

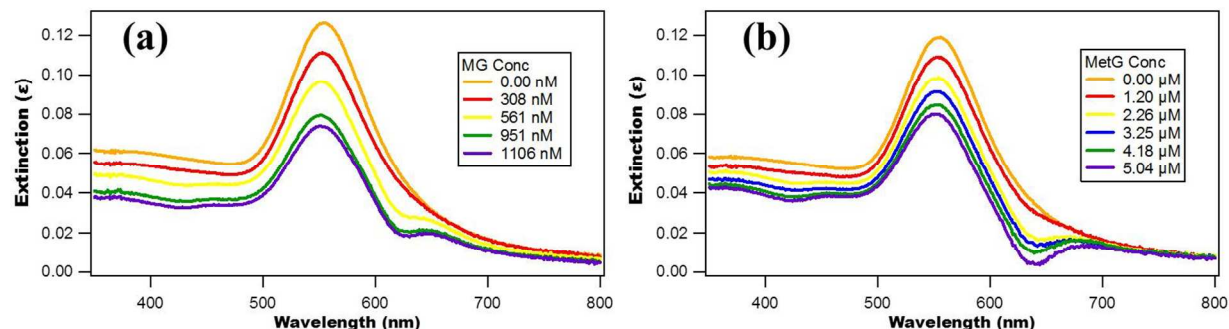


Figure S3. Extinction spectra of gold nanoparticles capped with MSA in water at different (a) malachite green and (b) methyl green concentrations after subtracted the corresponding spectra from the dye molecules alone in water. 0.30 mL of the 80.0 nm colloidal gold nanoparticles at a bulk concentration of  $4.1 \times 10^9$  nanoparticles/mL was added to 3.00 mL water.

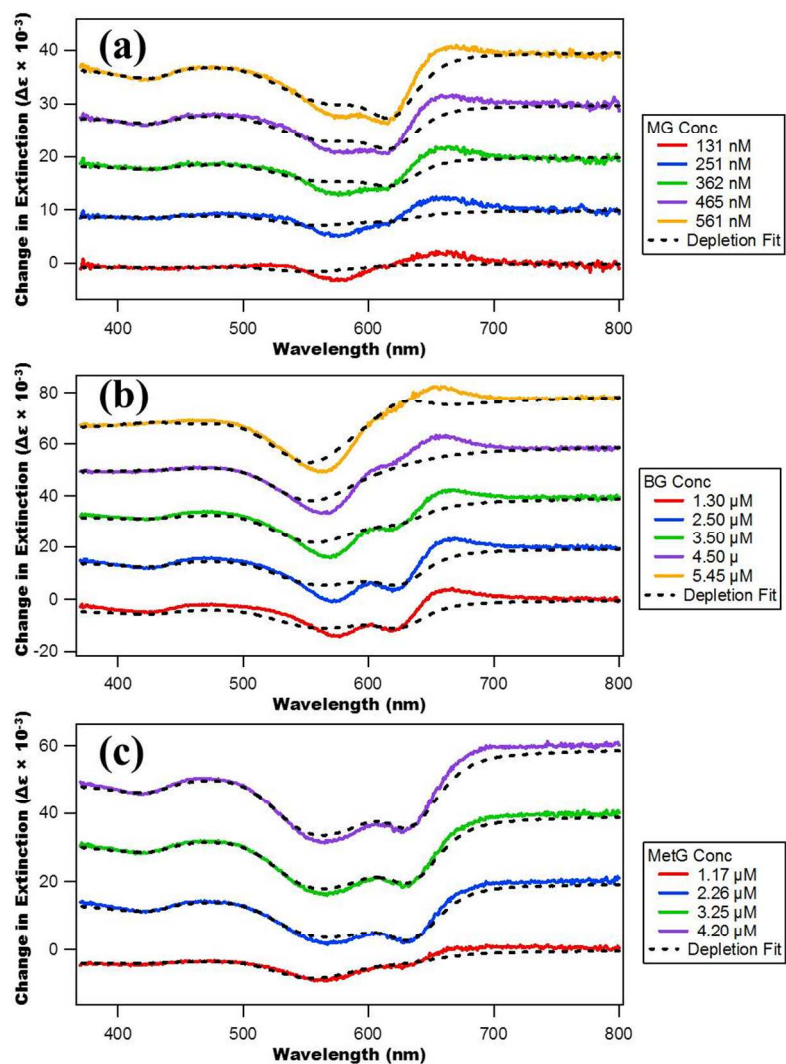


Figure S4. Change in extinction obtained from the subtraction of 80.0  $\pm$  6.1 nm gold nanoparticles capped with MSA in water ( $d = 9.1 \times 10^9$  nanoparticles per mL) and (a) different malachite green concentrations, (b) different brilliant green concentrations and (c) different methyl green concentrations in water from the spectra of a solution of dye and gold colloid (red solid line). The black dashed line corresponds to the best fit of the plasmon and molecule depletion peaks. A combination of Fano resonance and polaritons is observed. The spectra were offset for better comparison.

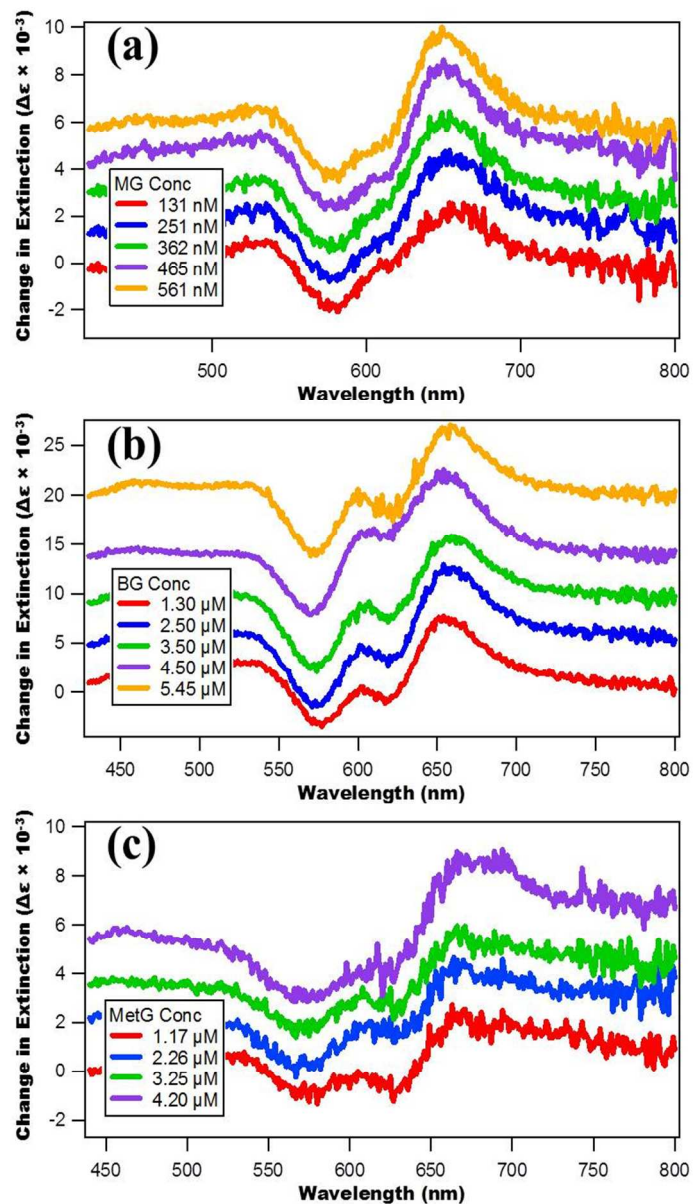


Figure S5. Spectra obtained after the subtraction of the depletion fit from the visible extinction difference spectra obtained from 80 nm gold nanoparticles at different dye concentrations (a) malachite green, (b) brilliant green, (c) methyl green in figure 5. The extra remaining peaks are due to a combination of polaritons and Fano resonance.

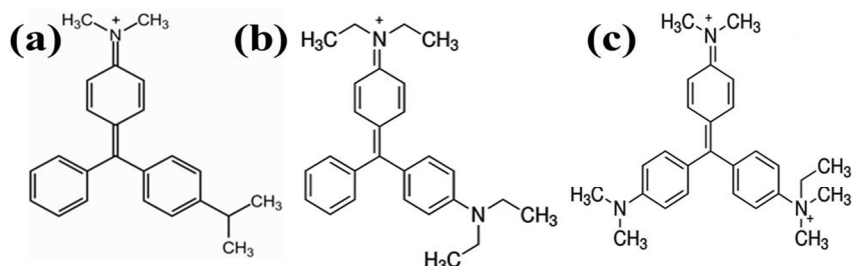


Figure S6. Chemical structures of the dye molecules: (a) malachite green, (b) brilliant green, and (c) methyl green.

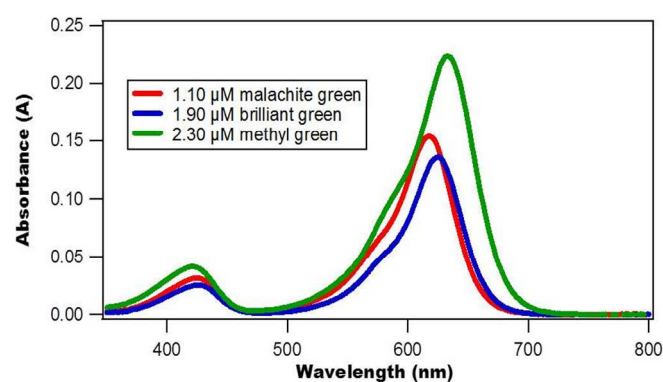


Figure S7. The absorption spectra of 1.1  $\mu\text{M}$  malachite green (red line), 1.9  $\mu\text{M}$  brilliant green (blue line), and 2.3  $\mu\text{M}$  methyl green (green line) in water.

#### REFERENCES:

- (1) Wang, H.; Yan, E.; Liu, Y.; Eienthal, K. B. Energetics and Population of Molecules at Microscopic Liquid and Solid Surfaces. *J. Phys. Chem. B* **1998**, *102*, 4446-4450
- (2) Haber, L. H.; Kwok, S.; Semeraro, M.; Eienthal, K. B. Probing the Colloidal Gold Nanoparticle/Aqueous Interface with Second Harmonic Generation. *Chem. Phys. Lett.* **2011**, *507*, 11-14